BIOCHEMISTRY
including biophysical chemistry & molecular biology

Article

pubs.acs.org/biochemistry

Intermediate Partitioning Kinetic Isotope Effects for the NIH Shift of 4-Hydroxyphenylpyruvate Dioxygenase and the Hydroxylation Reaction of Hydroxymandelate Synthase Reveal Mechanistic Complexity

Dhara D. Shah,[†] John A. Conrad,[‡] and Graham R. Moran*[,†]

[†]Department of Chemistry and Biochemistry, University of Wisconsin—Milwaukee, 3210 North Cramer Street, Milwaukee, Wisconsin 53211-3209, United States

[‡]Department of Chemistry, University of Nebraska—Omaha, 6001 Dodge Street, Omaha, Nebraska 68182-0109, United States

Supporting Information

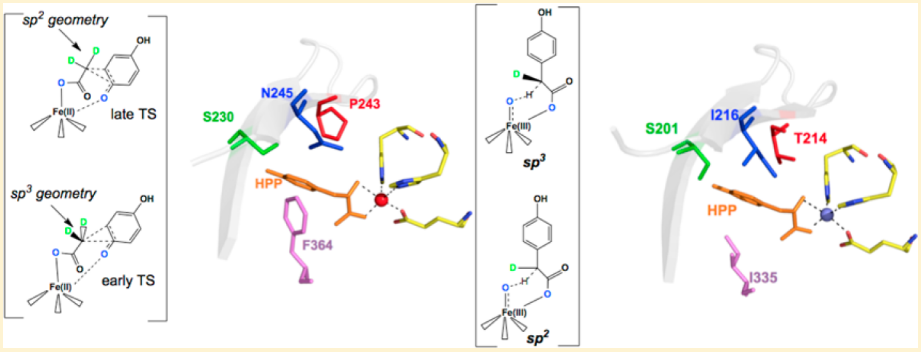

ABSTRACT: 4-Hydroxyphenylpyruvate dioxygenase (HPPD) and hydroxymandelate synthase (HMS) are similar enzymes that catalyze complex dioxygenation reactions using the substrates 4-hydroxyphenylpyruvate (HPP) and dioxygen. Both enzymes decarboxylate HPP and then hydroxylate the resulting hydroxyphenylacetate (HPA). The hydroxylation reaction catalyzed by HPPD displaces the aceto substituent of HPA in a 1,2-shift to form 2,5-dihydroxyphenylacetate (homogentisate, HG), whereas the hydroxylation reaction of HMS places a hydroxyl on the benzylic carbon forming 3′-hydroxyphenylacetate (*S*-hydroxymandelate, HMA) without ensuing chemistry. The wild-type form of HPPD and variants of both enzymes uncouple to form both native and non-native products. We have used intermediate partitioning to probe bifurcating steps that form these products by substituting deuteriums for protiums at the benzylic position of the HPP substrate. These substitutions result in altered ratios of products that can be used to calculate kinetic isotope effects (KIE) for the formation of a specific product. For HPPD, secondary normal KIEs indicate that cleavage of the bond in the displacement reaction prior to the shift occurs by a homolytic mechanism. NMR analysis of HG derived from HPPD reacting with enantiomerically pure *R*-3′-deutero-HPP indicates that no rotation about the bond to the radical occurs, suggesting that collapse of the biradical intermediate is rapid. The production of HMA was observed in HMS and HPPD variant reactions. HMS hydroxylates to form exclusively *S*-hydroxymandelate. When HMS is reacted with *R*-3′-deutero-HPP, the observed kinetic isotope effect represents geometry changes in the initial transition state for the nonabstracted proton. These data show evidence of sp^3 hybridization in a HPPD variant and sp^2 hybridization in HMS variants, suggesting that HMS stabilizes a more advanced transition state in order to catalyze H-atom abstraction.

4-Hydroxyphenylpyruvate dioxygenase (HPPD) and hydroxymandelate synthase (HMS) catalyze similar reactions using the same substrates, 4-hydroxyphenylpyruvate (HPP) and dioxygen. Initially, both enzymes reduce and activate dioxygen in order to decarboxylate HPP, yielding 4-hydroxyphenylacetate (HPA), CO_2, and an activated oxo intermediate.[1] Both enzymes then hydroxylate HPA but do so in different positions. HPPD catalyzes aromatic hydroxylation at the ring C1, resulting in a migration of the aceto group of HPA to yield 2,5-dihydroxyphenylacetate (homogentisate, HG), whereas HMS catalyzes hydroxylation of the HPA benzylic methylene to form S-hydroxymandelate (HMA) (Scheme 1). Despite modest sequence identity and similarity, the two enzymes clearly have a common ancestry in that they share numerous active site residues and adopt a highly similar fold.[2] HPPD is in all likelihood the progenitor because it is ostensibly ubiquitous in aerobes, where it catalyzes the second step of tyrosine

Received: April 29, 2013
Revised: July 18, 2013
Published: August 13, 2013

   dx.doi.org/10.1021/bi400534q | *Biochemistry* 2013, 52, 6097−6107

Scheme 1

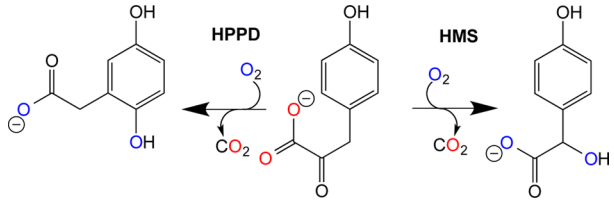

catabolism, whereas HMS catalyzes the first step in the biosynthesis of hydroxyphenylglycine, an uncommon tailoring reaction in a relatively small number of bacteria.[3,4]

Both HPPD and HMS are Fe(II)-dependent dioxygenases and, on the basis of the reactions they catalyze, can be grouped with the α-keto acid dependent oxygenases (α-KAOs).[5,6] Structurally, HPPD and HMS have no resemblance to other α-KAOs, so this classification is based solely on their chemical reactions.[7−9] α-KAOs catalyze an extraordinary range of chemistries; however, each member begins catalysis with the cleavage of dioxygen and the oxidative decarboxylation of an α-keto acid (almost universally α-ketoglutarate). These steps are thought to result in the formation of a common reactive intermediate (Fe(IV)═O) that is then directed to unique purposes by individual enzymes.[10−12] Although these purposes include an impressive array of oxidation reactions, halogenation, and even epimerization, this reactive oxo species is most often used to hydroxylate.[6] HPPD and HMS offer respective examples of aromatic and aliphatic hydroxylation chemistry in which the requisite α-keto acid is supplied by the pyruvate substituent of HPP rather than from α-ketoglutarate (Figure 1).

Aromatic hydroxylation by HPPD induces substituent migration. In the 1960s, Guroff et al. discovered that aromatic

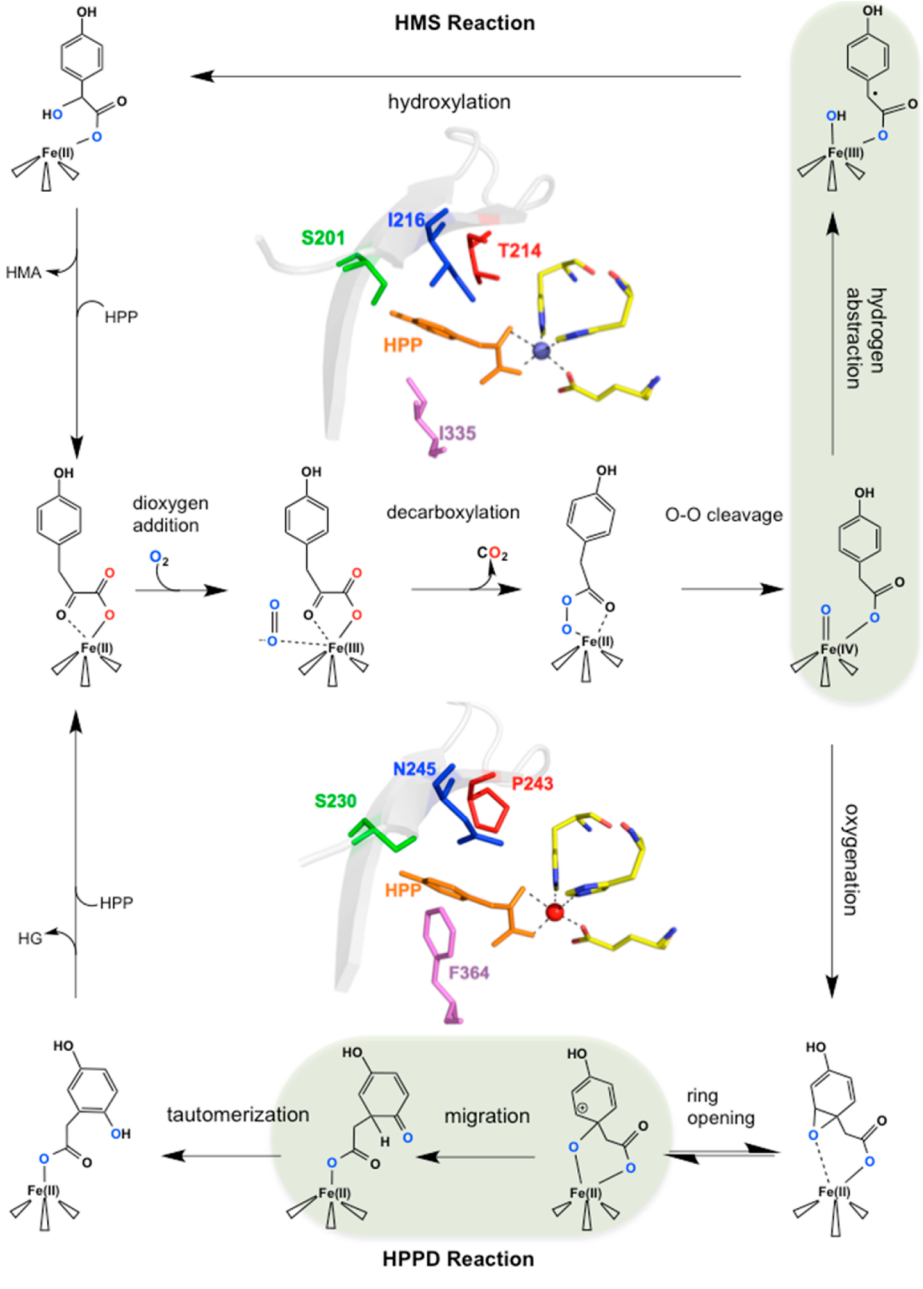

Figure 1.

dx.doi.org/10.1021/bi400534q | *Biochemistry* 2013, 52, 6097−6107

Scheme 2

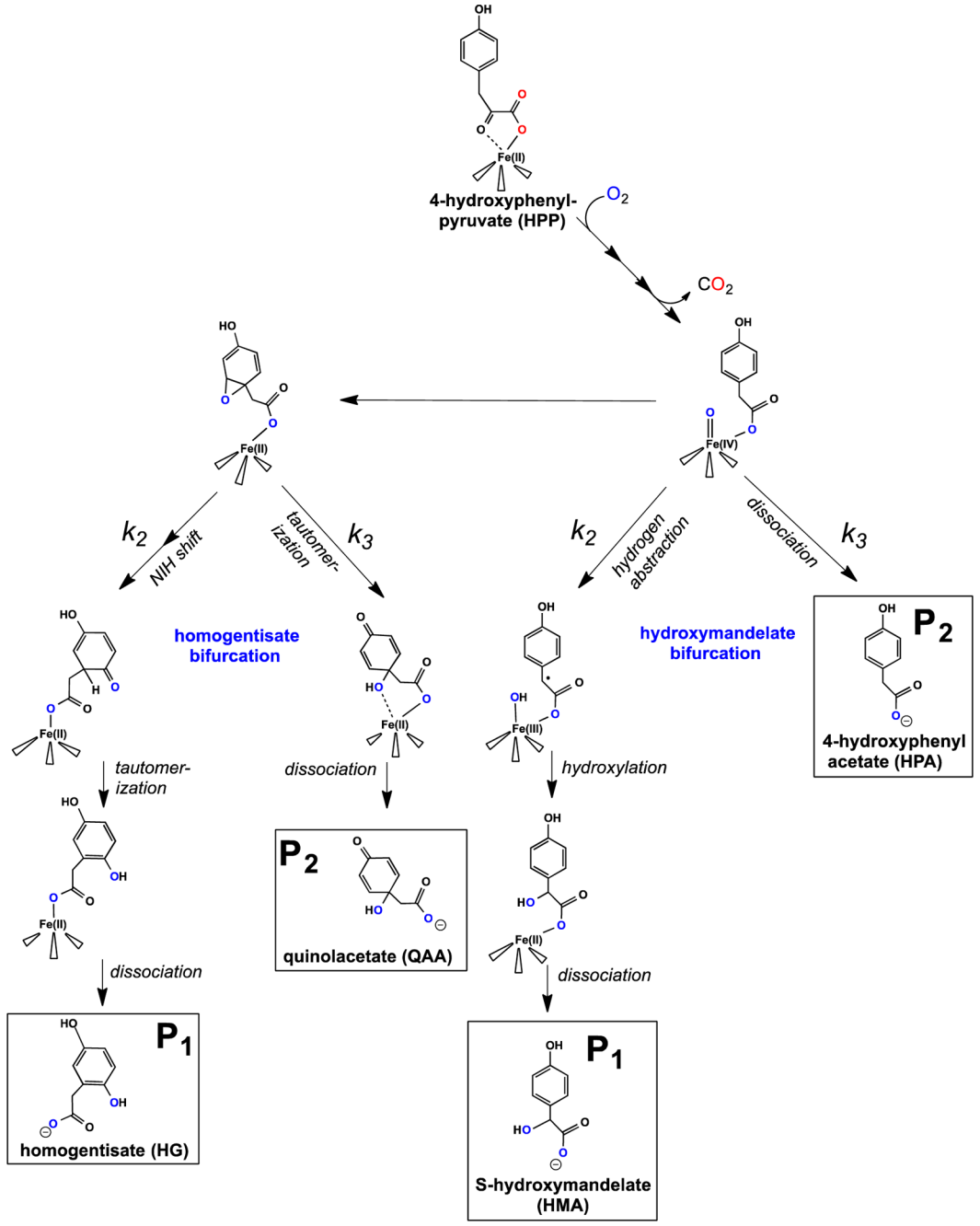

hydroxylation by pterin-dependent hydroxylases can induce an intramolecular migration or shift of the substituent from the site of hydroxylation.[13] Coined the *NIH shift*, this phenomenon has since been documented for a variety of metal-dependent oxygenases.[14−17] For essentially all, the shift is observed with compact substituents such as halides, deuteriums and tritiums (and presumably protiums), and methyl groups. It has also been observed that, for substituents larger than a proton, the shift occurs in only a fraction of total catalysis.[13,15,18−24] The aromatic hydroxylation reaction catalyzed by HPPD induces the migration of the comparatively large aceto substituent with high efficiency [25] and so, from an experimental standpoint, is an important example of this chemistry.

Initial attempts to define the mechanism of the HPPD shift used single enantiomer chiral monodeutero-HPP labeled at the benzylic carbon and subsequent configurational analysis of the product. It was contended that if a two-electron or carbanion mechanism was at work, sp^3 geometry at the benzylic carbon would predominate in the cleaved intermediate; therefore, a chiral substrate would retain the configuration in the product. Conversely, if the one-electron mechanism were operative, a symmetrical sp^2 in-flight radical could rotate before recombining with the ring, resulting in racemization at a chiral benzylic carbon. From these experiments, Leinberger et al. concluded that the NIH shift of HPPD occurred via a two-electron mechanism with retention of configuration at the benzylic methylene C atom.[22] More recently, using density functional approaches to compute the more probable of a comprehensive set of reaction coordinate possibilities, Borowski et al. concluded that the NIH shift of HPPD was likely to occur

dx.doi.org/10.1021/bi400534q | *Biochemistry* 2013, 52, 6097−6107

via a homolytic mechanism and that retention of configuration at the benzylic position was simply a consequence of a low barrier to the transition state (TS) for the displaced group to recombine with the ring relative to the barrier for bond rotation.[26] As such, there is some incongruity in the literature that is open to be settled by experimental observation that reports discriminating evidence for the mechanism of the NIH shift in HPPD.

The hydroxylation reaction catalyzed by HMS is less complex than that of HPPD and is thought to involve only an initial hydrogen abstraction by the Fe(IV)═O species from the benzylic position to form a benzylic radical followed by hydroxyl addition from the resulting Fe(III)—OH species.[25] Computational methods have provided a comprehensive description of the basis for hydroxylation regiospecificity in HMS and have suggested that H-atom abstraction forming a benzylic radical followed by oxygen rebound is the dominant mechanism.[27,28] Experimental evidence for the mechanism has come from kinetic isotope effect (KIE) values for the hydroxylation reaction from intermediate partitioning (vide infra) and were consistent with H-atom abstraction as the first step.[12,25,29]

The fundamental objectives of this study were to obtain experimental evidence that discriminates between the heterolytic and homolytic NIH-shift mechanisms with HPPD and to define the geometry of the benzylic radical that forms with H-atom abstraction in HMS (highlighted steps in Figure 1). The measurement of KIEs for the relevant catalytic steps would provide evidence for the mechanism(s), but for both HPPD and HMS, this observation cannot be made directly because the hydroxylation and NIH shift steps are kinetically shrouded in single turnover reactions.[30−32] We have recently shown that HPPD wild-type and also HPPD and HMS variants exhibit bifurcations that produce multiple products.[25] For HPPD, bifurcation at the NIH-shift step yields either quinolacetic acid (QAA), a molecule that is hydroxylated but has not undergone the shift, or the native shift product, HG,[25,33] whereas bifurcation for the H-atom abstraction step that forms HMA yields HPA, an intermediate that has undergone decarboxylation but is not hydroxylated [25] (Scheme 2). Thus, these systems are amenable to the measurement of intermediate-partitioning-based KIE values. The basis for this method is that the ratio of products is a direct result of a probability-based selection that is defined by the decay rate constant for individual paths bifurcating from some reactive state of the enzyme.[34] As such, substitutions of heavy isotopes for atoms that are involved in the chemistry of these diverging steps can alter the balance of the rate constants and thus the product ratio. Thus, an intrinsic kinetic isotope effect for a specific reaction step can be calculated simply. This accurate and highly robust method was originally applied to the P450 hydroxylases and more recently to mono- and dinuclear Fe(II) dependent oxygenases.[16,35−37] The data we have obtained via these methods give KIE values that are consistent with the mechanisms proposed for each of the catalytic steps, which at least narrows the mechanistic possibilities and suggests that alternate pathways can be induced that yield the same product in variant forms of the enzymes.

MATERIALS AND METHODS

Materials. HPP and HG were purchased from Acros Chemicals. HMA and 4-hydroxyphenylacetate (HPA) were obtained from Sigma-Aldrich. Phusion High-Fiedility PCR Master Mix and Competent BL21(DE3) *Escherichia coli* cells were obtained from New England Biolabs. IPTG was from Gold Biochemicals. D_2O and $CDCl_3$ were obtained from Cambridge Isotope Laboratories. DMSO-d_6 was from Acros Chemicals. The gene for mouse phenylpyruvate tautomerase (PPT) optimized for expression in *Escherichia coli* and including codons for a His-Tag was purchased from EnzymaX and subcloned into the Nde I and Xho I restriction sites of pET17b for expression. Q-Sepharose was from Bio-Rad. Sephacryl S-200 was obtained from Amersham. Quinolacetate (QAA) was made using the HPPD P243T variant and purified as previously described.[33] 3′,3′-Diduetero-HPP was prepared according to our previously published method.[32] Solutions of the enol form of HPP were prepared by dissolving crystalline enol-HPP (as purchased) in the aprotic water-miscible solvent methanol to prevent ketonization. The chiral shift reagent, rhombamine macrocycle, was a kind gift from Dr. Koichi Tanaka.[38] All other chemicals, buffers, and biological media were obtained from Fisher Scientific or Sigma-Aldrich Chemicals and were of high purity.

Mutagenesis. pET17b-derived (Novagen) plasmids carrying the *Streptomyces avermitilis* HPPD gene (pSAHPPD[39]) and the *Amycolatopsis orientalis* HMS gene (pAOHMS[2]) were mutated as previously described to obtain the N245Q, P243T, S230A, and N245S variants of HPPD and the S201A variant of HMS.[25,33] An additional HPPD variant for this study, F364I, was obtained using the Stratagene QuickChange protocol using Phusion High-Fidelity PCR Master Mix and the following oligonucleotides: TCGGCAAGGGCAACATCAAGGCCCT-GTTC paired with an oligonucleotide that was its reverse complement. All variants were screened for spurious mutations by sequencing the entire dioxygenase genes (Sequetech, Mountain View, CA).

Expression and Purification. The apo-forms of wild-type and variants of HPPD and HMS were expressed and purified using ammonium sulfate fractionation, anion exchange chromatography, and size exclusion chromatography according to published methods.[2,39]

His-tagged PPT was purified using the following protocol. Aliquots from frozen cell stocks were plated (200 μL/L of culture) on LB agar with 100 μg/mL ampicillin. After incubation for 9−12 h at 37 °C, the cells from two plates were suspended in ∼20 mL of LB broth and used to inoculate 1 L of LB broth with 100 μg/mL ampicillin. The culture was grown with vigorous shaking (225 rpm) at 37 °C until the cell density had reached an OD_{600} of 1.0. At this time, IPTG was added to a final concentration of 0.1 mM and incubation was continued for 2.5 h. The cells were harvested by centrifugation at 4665*g* for 30 min and used immediately for protein purification. Unless otherwise stated, all subsequent purification procedures were undertaken at 4 °C. Cells were resuspended using 20 mL of 20 mM HEPES, pH 7.0, per liter of culture and lysed with sonication (2 × 6 min at 45 W) using a Branson sonicator fitted with a blunt tungsten tip. The temperature of the solution was monitored to ensure that it did not exceed 10 °C. The lysed cells were then centrifuged at 15600*g* for 30 min, and the pellet was discarded. Streptomycin sulfate in water was then added to the supernatant to a final concentration of 1.5% w/v. The mixture was stirred for 10 min and centrifuged at 12900*g* for 15 min. The supernatant was then loaded directly onto a Talon metal affinity column pre-equilibrated in 20 mM HEPES, pH 7.0, at a flow rate of 1 mL/min. The column was washed with 20 mM HEPES and 10 mM imidazole, pH 7.0, to

dx.doi.org/10.1021/bi400534q | *Biochemistry* 2013, 52, 6097−6107

elute nonspecifically bound proteins. The PPT was eluted with a linear 600 mL gradient from 10 to 250 mM imidazole in 20 mM HEPES, pH 7.0, at a flow rate of 1 mL/min. The fractions containing PPT were pooled and stored at −80 °C.

KIE Values from HPLC Product Analysis. The ratio of products for wild-type and each variant enzyme were determined using high-pressure liquid chromatography (HPLC). Enzyme turnover reactions were undertaken at 25 °C and were composed of 25−30 μM ferrous sulfate, 10−20 μM enzyme (wild-type or variant HPPD or HMS), 1 mM reductant (either βME or ascorbic acid), 250 μM O_2, and 100−250 μM HPP (either 3′,3′-dideutero or diprotio) in 10 mM potassium phosphate, pH 7.0. Isotope effects were based on peak areas for products measured by HPLC as previously published.[25]

KIE values measured with *R*-3′-monodeutero-HPP were obtained from coupled turnover reactions in which the stereospecifically labeled monodeutero substrate was formed and consumed in situ. *R*-3′-monodeutero-HPP was prepared using phenylpyruvate tautomerase (PPT) in deuterium oxide solvent. PPT catalyzes a stereospecific reaction in which it interconverts the enol and keto forms of HPP by incorporating or abstracting a proton at the *pro-R* position.[40] The ratio of products observed for HPPD or HMS when *R*-3′-monodeutero-HPP was used as a substrate was determined by adding the enol form of HPP to a reaction that had both PPT and HMS or HPPD activities. The reaction was designed such that the combined PPT and nonenzymatic conversion of enol-HPP to *R*-3′-monodeutero-keto-HPP was 7-fold faster than the nonenzymatic conversion of the enol-HPP to the *S*-3′monodeutero-keto-HPP, and the HMS or HPPD activity was 4-fold greater than that of PPT, accounting for both the solvent kinetic isotope effect (SKIE) on the product release step of HPPD and HMS and the SKIE for PPT.[30,32,40,41] Enzyme turnover reactions were undertaken at 25 °C and were composed of ferrous sulfate equivalent to the concentration of HMS or HPPD that gave 1.06 U activity (12.5 μM S201A HMS or 106 μM F364I HPPD), 0.28 U of PPT, and 1 mM ascorbate in 5 mM sodium phosphate buffer prepared in deuterium oxide, pD 7.0 (U is a unit of enzyme activity and is equal to 1 μmol of substrate consumed or product evolved per min). The low concentration of buffer used in these reactions suppresses the observed rate constant for the nonenzymatic conversion of the enolic HPP to ketoic HPP. The reaction was initiated by the addition of 50 μM enol HPP in 100% methanol. After completion of the reaction, all other steps required to determine the product concentrations were as previously published.[25]

Calculation of KIEs. Kinetic isotope effects were calculated using eq 1, which computes the factor of perturbation of the product ratio in the presence of the deuterated substrate for the case of a bifurcating mechanism and incorporates a correction accounting for the fractional extent by which $^{D}k_{obs}$ is reduced from the intrinsic value ($^{D}k_2$) by the bifurcation.[34]

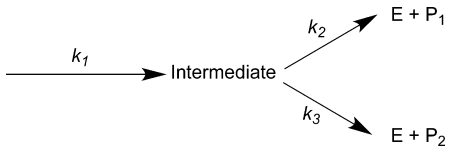

$$^{D}k_{obs} = \frac{(P_1/(P_1 + P_2))^{H}}{(P_1/(P_1 + P_2))^{D}} = \frac{^{D}k_2 + (k_2/k_3)}{1 + (k_2/k_3)} \quad (1)$$

In this equation, $^{D}k_{obs}$ is determined by measuring P_1, the concentration of product for which the isotope effect is being determined (HG or HMA for HPPD, and HMA for HMS), and P_2, the concentration of the product that results from bifurcation in a step that is insensitive to the isotopic insertion (QAA or HPA for HPPD, and HPA for HMS). In each measurement, the total consumption of molecular oxygen was compared to the total concentration of products formed to ensure that all catalysis was considered.

Preparation of Monodeuterated HG from Wild-Type HPPD. For the production of HG in sufficient quantity for NMR analysis, a large-scale turnover reaction (40 mL) was undertaken in D_2O with wild-type HPPD. The reaction mixture was composed of 420 U of wild-type HPPD, 112 U of PPT, 60 μM ferrous sulfate, and 1 mM ascorbate in 5 mM sodium phosphate buffer, pD 7.0, and was initiated with the addition of 1.5 mM enol HPP in methanol. The reaction was run at 25 °C and was equilibrated with 100% O_2 by stirring in a vessel with two small ports so that 100% dioxygen gas could continuously flush the headspace of the container. Complete conversion of the available HPP to HG was achieved within ∼40 min, as determined by analytical reversed-phase HPLC using published methods.[25] The reaction was then brought down to pD 2.0 by the addition of H_2SO_4 to stabilize the HG hydroquinone, and the precipitated protein was removed by centrifugation at 12900*g* for 20 min. The supernatant was then passed through 10 kDa nominal molecular weight limit centrifugal filter (Vivaspin15) by centrifuging at 3000*g* to remove residual soluble peptide. The filtrate was then lyophilized overnight to a volume of ∼5 mL, and the sample was loaded on to Sep-Pak Vac 35 cc C18 column pre-equilibrated with 40 mM sodium phosphate buffer, pH 7.0. The column was washed with 60 mL of H_2O, and the HG was then eluted with 10% acetonitrile in water. Each eluted fraction was examined spectrophotometrically for the characteristic λ_{max} absorbance of HG at 290 nm. Fractions showing significant absorbance at 290 nm were combined together and lyophilized to obtain dry (powdered) HG.

Chiral Shift Analysis of Monodeuterated HG. Lyophilized HG was dissolved in $CDCl_3$ containing 10% DMSO-d_6, from which 5 mg of HG was taken for NMR analysis. As a standard, a comparable amount of unlabeled HG solution in $CDCl_3$ containing 10% DMSO-d_6 was also prepared. Monodeuterated HG and unlabeled HG solutions were titrated with 0 to 0.05 equiv rhombamine macrocycle (chiral shift reagent) by small additions.[38] ^{1}H NMR spectra were recorded on a 500 MHz Bruker NMR instrument.

RESULTS

Product Analysis and Characterization of Variant Enzymes. All the HPPD and HMS variants except F364I HPPD and N245D HPPD have been characterized in prior work.[25] The product ratios for wild-type, N245Q, N245S, P243T, and S230A vary slightly from those previously published. However, the KIE values obtained by partitioning methods are calculated from a ratio of ratios and therefore are largely immune to such variation (eq 1). F364I HPPD and N245D HPPD could be expressed and purified using the same methods as wild-type HPPD.[39] Interestingly, F364I HPPD produced four products (Table 2), of which the most interesting was HMA, the product of the HMS reaction. This was consistent with the work of O'Hare et al. and Gunsior et al., who also observed HMA production with this variant.[42,43]

dx.doi.org/10.1021/bi400534q | *Biochemistry* 2013, 52, 6097−6107

Table 1. NIH Shift KIEs from Wild-Type HPPD and Variants[a]

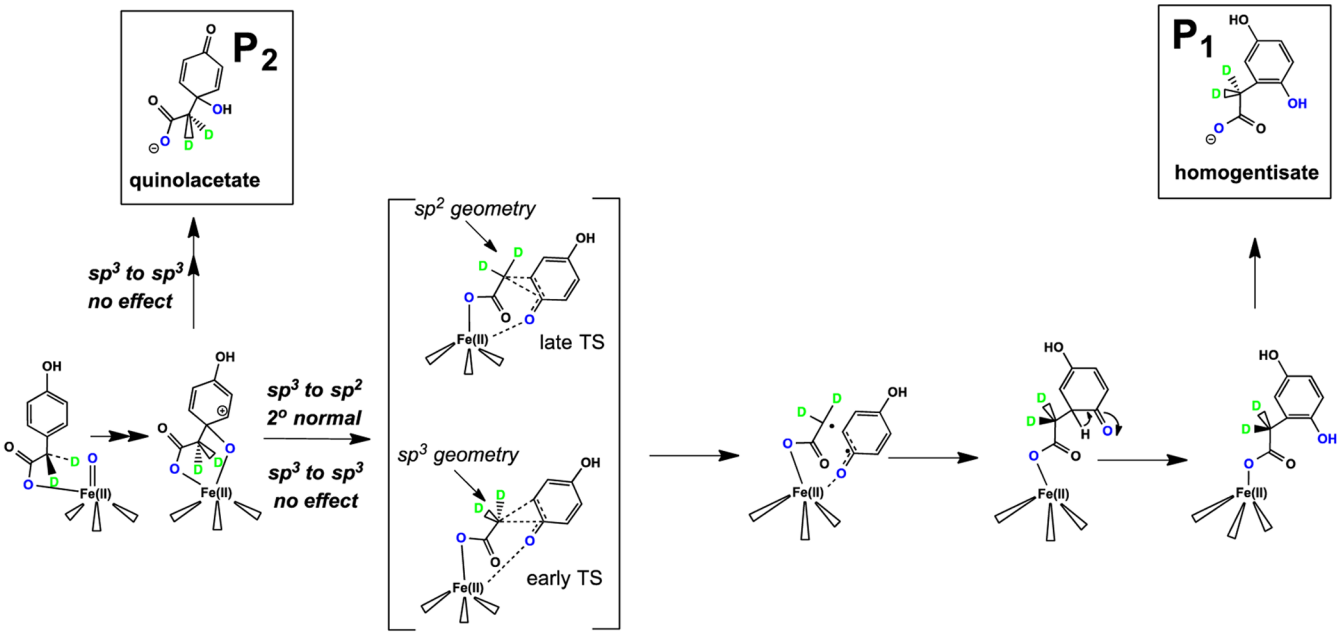

variant	wild-type	N245Q	N245D	N245S	P243T	S230A
HG (%)	90	52	52	3.4	8.4	7
QAA (%)	1	3	21.2	90	45	36
HPA (%)	9	45	26.8	6.6	46.5	57
$^{D}k_{obs}$ HG	0.990 ± 0.001	0.99 ± 0.03	1.03 ± 0.01	1.39 ± 0.02	1.08 ± 0.05	1.08 ± 0.01
replicates	2	2	2	2	2	2

[a]N.B. all product percentages are those obtained with the protio substrates. Product percentages for protio and deuteron substrates are available in the Supporting Information.

Although rationalizing the function of individual residues is secondary to the purpose of this study, it is interesting to note that the position occupied by F364 in the structure of HPPD is filled by I335 in the structure of HMS.[44] As such, this mutation yields one of the only single positional-switching variants for these two enzymes that has resulted in the alternate activity to any significant extent. N245D was a largely competent HPPD, successfully completing the NIH shift to form HG in 50% of total turnovers with the remaining fractions of turnover yielding QAA (20%) and HPA (30%).

KIEs for the NIH Shift from Intermediate Partitioning in Wild-Type and Variant HPPDs. Despite that HPPD catalysis represents one of the more compelling examples of shift chemistry, the NIH shift step neither contributes to the limiting rate of turnover nor is it resolved kinetically in single turnover reactions, so it is difficult to study by conventional methods.[30,31] Intermediate partitioning is one of the few experimental methods capable of providing direct evidence for the chemistry occurring in this step. Moreover, the precision obtained with this method is sufficient to discern between mechanisms based on KIEs of small magnitude, as are often obtained for secondary deuterium isotope effects arising from subtle hybridization changes at specific carbon atoms. Table 1 shows the utility of the product partitioning in differentiating between possible pathways for the NIH shift. For HPPD, QAA acts as an internal reference product for the shift step, having undergone hydroxylation but not the shift; thus, its formation rate constant would not be sensitive to deuterons placed at the benzylic carbon (C3′). To form HG, however, the enzyme must transiently sever the bond to this carbon, so the rate constant for the formation of HG will reflect an extent of influence of benzylic deuterons (Scheme 2). Wild-type HPPD and variant N245Q show a KIE of 1 for the formation of the native product HG, which indicates that no significant geometric change at C3′ occurs in the formation of the (first) TS for the shift, or more precisely that the sp^3 geometry predominates. The interpretation of this number does not converge on a single mechanism. A trigonal C3′ in the shift TS is consistent with an early TS that has retained much of the initial hybridization of the preshift benzylic methylene. It does not, however, indicate explicitly that the mechanism is hetero- or homolytic, as the TS could readily progress to either an in-flight radical or carbanion intermediate.

In contrast, N245S HPPD showed a distinctly normal KIE of 1.39. This indicates that the (net) rate constant leading the formation of HG for this variant is slowed by deuterons in the benzylic position and that a transient geometry change at C3′ must accompany the formation of the shift TS. An sp^3 to sp^2 hybridization change resulting from homolytic severing of the C1−C3′ bond would account for the observed effect with this variant, suggesting a later TS in which the unrestrained in-flight radical character (sp^2) is developed in the TS.

Taken together, and assuming that the reaction traverses the same barrier for both wild-type and variants, these data support homolytic cleavage of the bond to the methylene attending the NIH shift. This conclusion is consistent with what has been proposed by Borowski et al. who, from calculation, also proposed a highly unstable biradical intermediate resulting from the severed bond that collapses to form the new bond to the ring.[26] All other HPPD variants tested in this manner, N245D,

dx.doi.org/10.1021/bi400534q | Biochemistry 2013, 52, 6097−6107

Table 2. Delineation of KIE for the Formation of HMA To Identify Hybridization Geometry of the Radical[a]

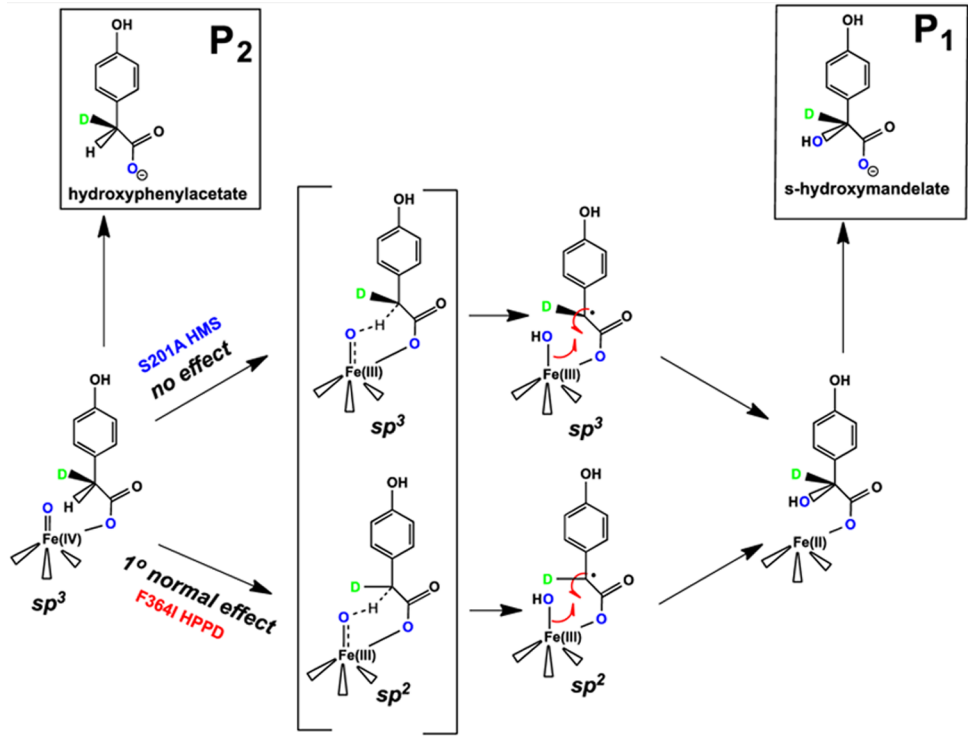

variant	F364I HPPD	S201A HMS
HG (%)	47	0
QAA (%)	19	0
HPA (%)	15	3
HMA (%)	20	97
total (%)	100	100
$^{D}k_{obs}$, 3′,3′-dideutero-HPP	3.52 ± 0.1	2.020 ± 0.004
replicates	2	3
$^{D}k_{obs}$ *R*-3′-monodeutero-HPP	1.92 ± 0.16	1.06 ± 0.04
replicates	2	3

[a]N.B. all product percentages are those obtained with the protio substrates. Product percentages for protio and deutero substrates are available in the Supporting Information.

P243T, and S230A, show small secondary normal KIEs (1.03−1.08) for the formation of HG. Within error, these values suggest shift TS geometry similar to the wild-type (C3′-sp^3).

NMR Chiral Shift Analysis of 3′-Monodeutero-HG. To further add to our evidence for the nature of the NIH shift chemistry, we examined the native product, HG, for evidence of deuterium scrambling when derived from stereospecifically labeled HPP (*R*-3′-monodeutero). This experiment was undertaken simply to reaffirm the observations of Leinberger et al., who conceded that derivatization of the product may have influenced the degree of scrambling observed.[22] The hypothesis for this experiment is that heterolytic cleavage of the C1−C3′ bond would disfavor racemization of the label at C3′ due to the polar trigonal shape of the in-flight carbanion, whereas the inherently planar and symmetrical sp^2 radical in this position could permit scrambling. Figure 2 shows NMR spectra that depict a titration of HPPD-derived monodeuterated HG with rhombamine macrocycle chiral shift reagent.[38] In this figure, inset spectra in blue are for unlabeled HG. The lower of these standard spectra is without shift reagent and shows a single shift for the equivalent benzylic protons. The upper standard spectrum shows splitting of these two benzylic protons in an AB spin system with the addition of the shift reagent. The spectra in black include the titration of the HPPD-derived HG with the shift reagent. In the absence of the shift reagent, two HG populations are observed: One resonates at 3.34 ppm and corresponds to the benzylic protons of unlabeled HG. The second resonance at 3.32 ppm is for *R*- or *S*- and/or *RS*-3′-monodeutero-HG. The greatest extent of splitting for unlabeled HG was observed for 0.035 equiv of the shift reagent; however, HPPD derived monodeutero-HG does not show evidence of splitting indicating a single enantiomer of monodeuterated HG. It can now be stated that this lack of label scrambling is indeed *characteristic* to the reaction. However, as noted by Borowski et al., this evidence by itself is not discriminating for the chemistry of the shift. Such a result would be predicted for the heterolytic pathway but is also equally consistent with a homolytic pathway in which the collapse of a biradical intermediate occurs orders of magnitude more rapidly than the time taken for a C2′−C3′ bond rotation.[26]

Deconstruction of Net KIE Values for the Production of HMA Using Stereospecifically Deuterated HPP. In prior work, we have measured the primary deuterium KIE on

dx.doi.org/10.1021/bi400534q | *Biochemistry* 2013, 52, 6097−6107

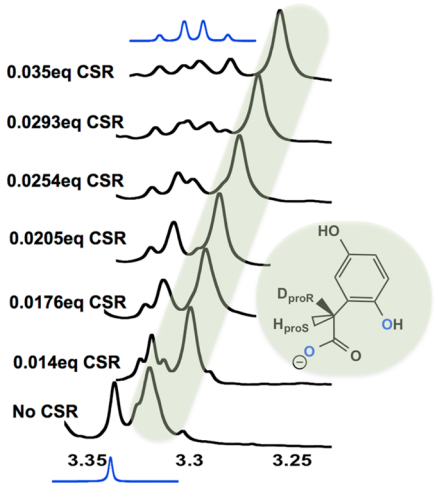

Figure 2. Evidence for a single enantiomer of homogentisate derived from *R*-3′-deutero-4-hydroxyphenylpyruvate. HG (5 mg) derived from HPPD reacting with *R*-3′-monodeutero-HPP was dissolved in $CDCl_3$ and 10% DMSO-d_6. A comparable amount of unlabeled HG solution in $CDCl_3$ containing 10% DMSO-d_6 was also prepared. Monodeuterated HG and unlabeled HG solutions were titrated with 0 to 0.05 equiv rhombamine macrocycle (chiral shift reagent) by small additions. ^{1}H NMR spectra were recorded on a 500 MHz Bruker NMR instrument. Blue spectra show the spectra of 3′-diprotic HG in the presence and absence of the chiral shift reagent.

the initial hydrogen abstraction step of the hydroxylation reaction for HMS using 3′,3′-dideutero-HPP.[25] Although the value measured was modest (2.2−2.6 depending on the enzyme variant), it includes a multiplicative component from the geometry at the benzylic carbon for the deuteron not in-flight (Table 2). Two variants were selected to measure KIEs for the production of HMA with *R*-3′-monodeutero-HPP. The first was S201A HMS and the second was F364I HPPD (that makes 20% HMA). Table 2 includes the percentage of each product produced by these variants and KIEs measured for the formation of HMA with 3′,3′-dideutero-HPP as well as 3′-*R*-monodeuterated HPP. With 3′,3′-dideutero-HPP as a substrate, S201A HMS and F364I HPPD show combined primary/secondary KIEs of 2.02 and 3.52, respectively. For KIEs measured with 3′-*R*-monodeuterated HPP as a substrate, S201A HMS showed a value of 1.06 ± 0.04 for the production of HMA, indicating the benzylic carbon retains predominant sp^3 character in the TS for the initial hydrogen abstraction. Conversely for F364I HPPD, the secondary KIE measured with 3′-*R*-monodeuterated HPP for the formation of HMA was 1.92 ± 0.16, indicating that a geometry change accompanies benzylic hydrogen abstraction for this HPPD variant. This would be consistent with a change from sp^3 to sp^2 geometry in the TS for this step.

DISCUSSION

Both HPPD and HMS have been studied in single turnover reactions in some detail.[30−32] Although both enzymes accumulate multiple transients, none of the steps observed show sensitivity to isotopic substitutions at positions of the substrate that are involved in hydroxylation.[30] As such, it was concluded that the hydroxylation steps of the catalytic cycle were fast relative to other steps, so the reactive species involved could not be observed directly by kinetic methods. Recently, we have shown that active site variants of both enzymes can form alternate products in some fraction of the total turnover.[25,33] Although it may be tempting to rationalize the meaning of the ratios of products observed with regard to the function of specific residues, the ratios are dependent on the prevailing conditions of the reaction (data not shown) and therefore offer limited opportunities for meaningful conclusions. However, multiple products indicate that bifurcations (and trifurcations) are occurring at identifiable stages of catalysis. Specific heavy isotope substitutions therefore have the potential to alter the rate constant associated with one arm of the bifurcation; as such, the KIE for that step can be calculated if the other arm of the branch is unaffected by the substitution (eq 1, Scheme 2). Although the data obtained by such methods can be exceedingly precise, they are also easily overinterpreted. The inherent kinetic complexity of a multiproduct system dictates that rationalization of results will likely offer explanations that are narrow relative to all possible mechanistic and kinetic possibilities. Herein, we have attempted to explain our data primarily on the basis of geometric changes in the transition state of the step affected by the isotope substitution. This approach assumes that the individual steps are largely irreversible or that their commitment forward is such that any reversibility can be ignored. This is broadly reasonable because oxygenases catalyze highly exothermic reactions for which most steps will be irreversible or committed forward. Reversibility is only relevant for those steps that define the ratio of products of interest (i.e., for the initial steps that lead from the branch point to the products that define the KIE value). Reversibility in either of the steps leading away from bifurcating intermediate will increase the proportion of the other product independent of the TS geometry. Thus, it should be noted that the assumptions upon which conclusions are based in this study cannot, in the absence of additional data, be validated, so what follows is a confined set of conclusions that attempt to form a reasoned explanation for the observations but cannot account exhaustively for the nuanced nature of the interpretation of individual KIE values for complex systems.

In our earlier work using similar methods, we measured KIE values on the ring-oxygen insertion step for HPPD using ring-per-deutero-HPP and, on the hydrogen abstraction step of HMS, using 3′,3′-dideutero-HPP. We observed an inverse secondary isotope effect for ring hydroxylation in HPPD that is consistent with the formation of an epoxide as the initial product of oxygen addition to the aromatic ring. For HMS, abstraction of the *S*-deuteron from HPP dideuterated at the benzylic position gave a normal primary effect consistent with H-atom abstraction before hydroxylation [25] (Figure 1). In the present study, we have again investigated one branch point for each enzyme (Scheme 2). For HPPD, we have studied a branch point beyond ring-oxygen insertion from which either the native product HG or QAA is formed. This branch was probed using 3′,3′-dideutero-HPP to examine if the formation rate constant for HG is influenced by geometric changes at the benzylic carbon during the NIH shift. The shift reaction was further studied using *R*-3′-monodeutero-HPP to detect evidence of racemization at the benzylic carbon during the aceto group migration. For HMS, we have expanded our prior investigation of the hydroxylation step with the use of *R*-3′-monodeutero-HPP. The single enantiomer of the substrate permitted the measurement of the contribution from the nonabstracted deuteron to the KIE value measured for HMS variants in prior work and therefore has provided evidence for

dx.doi.org/10.1021/bi400534q | *Biochemistry* 2013, 52, 6097−6107

the hybridization state at the benzylic carbon atom in the TS for the step that precedes hydroxylation.

The hydroxylation/shift reaction of HPPD has long been a biochemical curiosity and has been investigated using experimental and computational methods. The earliest direct evidence for the chemistry of the shift in HPPD came from Leinberger et al., who were able to show that the configuration of the benzylic carbon was retained during the shift and proposed that a two-electron process (heterolytic pathway) was at work.[22] The conclusions made here differ from those of Leinberger. Our KIE data show that no isotope effect is observed for the formation of HG when 3′,3′-dideutero-HPP is used as a substrate (Table 1). Although this alone could be said to be consistent with a TS leading to a benzylic carbanion (sp^3) intermediate, it is also consistent with an sp^3 hybridized TS that exhibits little of the character of an ensuing sp^2 hybridized intermediate (i.e., an early TS). The more definitive observation is the KIE value measured for this branch with the N245S variant, which is distinctly normal (1.4). If we accept that the mechanism is conserved between the wild-type and variant, this value represents a more mature TS in which the benzylic methylene is largely departed from the ring C1 and has adopted the geometry of an untethered radical (sp^2) (scheme in Table 1).

Leinberger et al. showed both that configuration at the benzylic position was retained and that the product HG was not racemized to any measurable extent.[22] This important work established a fundamental facet of HPPD chemistry. However, the methods chosen required derivatization of HG in order to compare the chirality with synthesized chirality standards, undermining to some extent the certainty of the observation. In order to solidify the conclusions regarding racemization during the NIH shift, we repeated the scrambling experiments of Leinberger et al. using a chiral shift reagent to induce chirality, a method that has the advantage of not chemically altering the product. Our data confirm the earlier observations that the monodeuterated HG formed in the reaction of HPPD with *R*-3′-monodeutero-HPP is a single enantiomer, so we conclude simply that bond rotation does not occur during the migration step (Figure 2). Borowski et al. have proposed that the NIH shift occurs through a homolytic pathway that does not induce racemization due to a relatively high barrier for bond rotation compared to that of the radical collapse that forms the new substituent bond.[26] The integrated conclusion is thus in agreement with that of Borowski and suggests homolytic cleavage in the first shift TS followed by the facile collapse of a biradical intermediate.

Partitioning KIEs measured with deuteriums substituted at the benzylic carbon of HPP for S201A HMS and F364I HPPD for the product HMA report the geometry of the H-atom abstraction TS. Our data indicate that these variants undergo different geometry changes at the benzylic carbon during the initial H-atom abstraction. KIE values measured using 3′,3′-dideutero-HPP are multiplicative for the hydrogen abstracted and the hydrogen retained and thus are expected to be greater than KIE values measured with *R*-3′-monodeuterated HPP (given that inverse effects are not predicted). Wojcik et al. and Neidig et al. both concluded from density functional approaches that the HMS hydroxylation chemistry involves H-atom abstraction leading to formation of a largely planar (predominately sp^2) benzylic radical.[27,28] Our conclusions regarding this step deviate only slightly from these prior determinations. The measured KIEs for HMA formation with both HPPD (F364I) and HMS (S201A) are internally consistent in that each value determined with the monodeuterated substrate is smaller than the value recorded with the 3′,3′-dideutero substrate. For S201A HMS, KIE values with 3′,3′-dideutero-HPP are higher than with *R*-3′-monodeutero-HPP by a factor of 2, indicating a primary KIE for abstraction, which suggests a more optimized benzylic hydroxylation process in HMS compared to that of the HPPD F364I variant. However, the KIE obtained with *R*-3′-monodeutero-HPP is, within error, unity; this indicates that the benzylic carbon does not change geometry significantly to reach the hydrogen abstraction TS. The conclusion in this case is that the TS for this step has sp^3 character at C3′. Interestingly, Wojcik et al. proposed that the S201 residue is vital for hydroxylation regiospecificity by tethering the phenol of HPA at unique angles in HPPD and HMS, so mutation of this residue may have resulted in a change in geometry in the abstraction TS.[27] For F364I HPPD, the KIE values for H-atom abstraction TS are 1.83 for hydrogen abstraction and 1.92 for geometry changes at the benzylic carbon in this step, suggesting that the benzylic carbon develops predominant sp^2 character with relatively little lengthening of the bond to the abstracted hydrogen in the TS. These values are in line with the prior modeling studies and raise the possibility for redundancy in the chemistry, where the dominant chemistry is to form a TS that is largely sp^2 hybridized at C3′, but an HMS variant can be made to exhibit sp^3 character at this position for the TS of this step and yet yield the same product.

■ ASSOCIATED CONTENT

Supporting Information

Product ratios from which KIE values were derived. This material is available free of charge via the Internet at http://pubs.acs.org.

■ AUTHOR INFORMATION

Corresponding Author

*G. R. Moran: e-mail, moran@uwm.edu; phone, (414) 229 5031; fax, (414) 229 5530.

Funding

This research was supported by a National Science Foundation grant to G.R.M. (MCB0843619) and by a UWM Research Growth Initiative grant to G.R.M.

Notes

The authors declare no competing financial interest.

■ ACKNOWLEDGMENTS

We would like to express our gratitude to Dr. Kiochi Tanaka of Kansai University, Osaka, Japan, for supplying the rhombamine macrocycle used as a chiral shift reagent for NMR analysis of homogentiste. These are an exceptional collection of molecules that allow chirality determinations of aromatic acids. We are also grateful to Holger Forsterling of the University of Wisconsin−Milwaukee for his continued assistance with operation of the 500 MHz NMR spectrometer.

■ ABBREVIATIONS

HPPD, 4-hydroxyphenylpyruvate dioxygenase; HPP, 4-hydroxyphenylpyruvate; HG, 2,5-dihydroxyphenylacetate, homogentisate; QAA, quinolacetic acid; HMS, hydroxymandelate synthase; HMA, hydroxymandelate; HPA, 4-hydroxyphenylacetate; α-KAO, α-keto acid-dependent oxygenase; βME, β-

mercaptoethanol; NIH, National Institutes of Health; KIE, kinetic isotope effect; HPLC, high-pressure liquid chromatography; PPT, phenylpyruvate tautomerase; NMR, nuclear magenetic resonance

REFERENCES

(1) Diebold, A. R., Brown-Marshall, C. D., Neidig, M. L., Brownlee, J. M., Moran, G. R., and Solomon, E. I. (2011) Activation of alpha-Keto Acid-Dependent Dioxygenases: Application of an {FeNO}(7)/{FeO(2)}(8) Methodology for Characterizing the Initial Steps of O(2) Activation. *J. Am. Chem. Soc. 133*, 18148−18160.

(2) Brownlee, J., He, P., Moran, G. R., and Harrison, D. H. (2008) Two roads diverged: the structure of hydroxymandelate synthase from Amycolatopsis orientalis in complex with 4-hydroxymandelate. *Biochemistry 47*, 2002−2013.

(3) Hubbard, B. K., Thomas, M. G., and Walsh, C. T. (2000) Biosynthesis of L-p-hydroxyphenylglycine, a non-proteinogenic amino acid constituent of peptide antibiotics. *Chem. Biol. 7*, 931−942.

(4) Li, T. L., Choroba, O. W., Charles, E. H., Sandercock, A. M., Williams, D. H., and Spencer, J. B. (2001) Characterisation of a hydroxymandelate oxidase involved in the biosynthesis of two unusual amino acids occurring in the vancomycin group of antibiotics. *Chem. Comm. (Cambridge, England)*, 1752−1753.

(5) Hausinger, R. P. (2004) FeII/alpha-ketoglutarate-dependent hydroxylases and related enzymes. *Crit. Rev. Biochem. Mol. Biol. 39*, 21−68.

(6) Purpero, V., and Moran, G. R. (2007) The diverse and pervasive chemistries of the alpha-keto acid dependent enzymes. *JBIC 12*, 587−601.

(7) Armstrong, R. N. (2000) Mechanistic diversity in a metalloenzyme superfamily. *Biochemistry 39*, 13625−13632.

(8) He, P., and Moran, G. R. (2011) Structural and mechanistic comparisons of the metal-binding members of the vicinal oxygen chelate (VOC) superfamily. *J. Inorg. Biochem. 105*, 1259−1272.

(9) Zhang, Z., Ren, J., Harlos, K., McKinnon, C. H., Clifton, I. J., and Schofield, C. J. (2002) Crystal structure of a clavaminate synthase-Fe(II)-2-oxoglutarate- substrate-NO complex: evidence for metal centred rearrangements. *FEBS Lett. 517*, 7−12.

(10) Price, J. C., Barr, E. W., Glass, T. E., Krebs, C., and Bollinger, J. M., Jr. (2003) Evidence for hydrogen abstraction from C1 of taurine by the high-spin Fe(IV) intermediate detected during oxygen activation by taurine:alpha-ketoglutarate dioxygenase (TauD). *J. Am. Chem. Soc. 125*, 13008−13009.

(11) Galonic, D. P., Barr, E. W., Walsh, C. T., Bollinger, J. M., Jr., and Krebs, C. (2007) Two interconverting Fe(IV) intermediates in aliphatic chlorination by the halogenase CytC3. *Nat. Chem. Biol. 3*, 113−116.

(12) Hoffart, L. M., Barr, E. W., Guyer, R. B., Bollinger, J. M., Jr., and Krebs, C. (2006) Direct spectroscopic detection of a C-H-cleaving high-spin Fe(IV) complex in a prolyl-4-hydroxylase. *Proc. Natl. Acad. Sci. U. S. A. 103*, 14738−14743.

(13) Guroff, G., Daly, J. W., Jerina, D. M., Renson, J., Witkop, B., and Udenfriend, S. (1967) Hydroxylation-induced migration: The NIH shift. *Science 157*, 1524−1530.

(14) Hillas, P. J., and Fitzpatrick, P. F. (1996) A mechanism for hydroxylation by tyrosine hydroxylase based on partitioning of substituted phenylalanines. *Biochemistry 35*, 6969−6975.

(15) Moran, G. R., Derecskei-Kovacs, A., Hillas, P. J., and Fitzpatrick, P. F. (2000) On the Catalytic Mechanism of Tryptophan Hydroxylase. *J. Am. Chem. Soc. 122*, 4535−4541.

(16) Mitchell, K. H., Rogge, C. E., Gierahn, T., and Fox, B. G. (2003) Insight into the mechanism of aromatic hydroxylation by toluene 4-monooxygenase by use of specifically deuterated toluene and p-xylene. *Proc. Natl. Acad. Sci. U. S. A. 100*, 3784−3789.

(17) Sono, M., Roach, M. P., Coulter, E. D., and Dawson, J. H. (1996) Heme-containing oxygenases. *Chem. Rev. 96*, 2841−2888.

(18) Jerina, D. M., Daly, J. W., and Witkop, B. (1968) The role of arene oxide-oxepin systems in the metabolism of aromatic substrates. II. Synthesis of 3,4-toluene-4−2H oxide and subsequent ″NIH shift″ to 4-hydroxytoluene-3−2H. *J. Am. Chem. Soc. 90*, 6523−6525.

(19) Jerina, D. M., Daly, J. W., and Witkop, B. (1971) Migration of Substituents during Hydroxylation of Aromatic Substrates (NIH Shift). Oxidations with Peroxytrifluoroacetic Acid. *Biochemistry 10*, 366−372.

(20) Daly, J. W., Jerina, D. M., and Witkop, B. (1972) Arene oxides and the NIH shift: The metabolism, toxicity and carcinogenicity of aromatic compounds. *Experientia 28*, 1129−1264.

(21) Bowman, W. R., Gretton, W. R., and Kirby, G. W. (1980) Hydroxylation of phenylalanine by Pseudomonas sp.: Measurement of an isotope effect following the NIH shift. *Perkin Trans. 1 (1972−1999) 3*, 218−220.

(22) Leinberger, R., Hull, W. E., Simon, H., and Retey, J. (1981) Steric course of the NIH shift in the enzymic formation of homogentisic acid. *Eur. J. Biochem. 117*, 311−318.

(23) Moran, G. R., Phillips, R. S., and Fitzpatrick, P. F. (1999) Influence of steric bulk and electrostatics on the hydroxylation regiospecificity of tryptophan hydroxylase: characterization of methyltryptophans and azatryptophans as substrates. *Biochemistry 38*, 16283−16289.

(24) Hillas, P. J., and Fitzpatrick, P. F. (1996) A mechanism for hydroxylation by tyrosine hydroxylase based on partitioning of substituted phenylalanines. *Biochemistry 35*, 6969−6975.

(25) Shah, D. D., Conrad, J. A., Heinz, B., Brownlee, J. M., and Moran, G. R. (2011) Evidence for the mechanism of hydroxylation by 4-hydroxyphenylpyruvate dioxygenase and hydroxymandelate synthase from intermediate partitioning in active site variants. *Biochemistry 50*, 7694−7704.

(26) Borowski, T., Bassan, A., and Siegbahn, P. E. M. (2004) 4-hydroxyphenylpyruvate dioxygenase: A hybrid density functional study of the catalytic reaction mechanism. *Biochemistry 43*, 12331−12342.

(27) Wojcik, A., Broclawik, E., Siegbahn, P. E., and Borowski, T. (2012) Mechanism of benzylic hydroxylation by 4-hydroxymandelate synthase. A computational study. *Biochemistry 51*, 9570−9580.

(28) Neidig, M. L., Decker, A., Choroba, O. W., Huang, F., Kavana, M., Moran, G. R., Spencer, J. B., and Solomon, E. I. (2006) Spectroscopic and electronic structure studies of aromatic electrophilic attack and hydrogen-atom abstraction by non-heme iron enzymes. *Proc. Natl. Acad. Sci. U. S. A. 103*, 12966−12973.

(29) Price, J. C., Barr, E. W., Hoffart, L. M., Krebs, C., and Bollinger, J. M., Jr. (2005) Kinetic Dissection of the Catalytic Mechanism of Taurine:alpha-Ketoglutarate Dioxygenase (TauD) from Escherichia coli. *Biochemistry 44*, 8138−8147.

(30) Johnson-Winters, K., Purpero, V. M., Kavana, M., and Moran, G. R. (2005) Accumulation of Multiple Intermediates in the Catalytic Cycle of (4-Hydroxyphenyl)pyruvate Dioxygenase from Streptomyces avermitilis. *Biochemistry 44*, 7189−7199.

(31) Purpero, V. M., and Moran, G. R. (2006) Catalytic, noncatalytic, and inhibitory phenomena: kinetic analysis of (4-hydroxyphenyl)-pyruvate dioxygenase from Arabidopsis thaliana. *Biochemistry 45*, 6044−6055.

(32) He, P., Conrad, J. A., and Moran, G. R. (2010) The rate-limiting catalytic steps of hydroxymandelate synthase from Amycolatopsis orientalis. *Biochemistry 49*, 1998−2007.

(33) Brownlee, J. M., Heinz, B., Bates, J., and Moran, G. R. (2010) Product analysis and inhibition studies of a causative Asn to Ser variant of 4-hydroxyphenylpyruvate dioxygenase suggest a simple route to the treatment of Hawkinsinuria. *Biochemistry 49*, 7218−7226.

(34) Fitzpatrick, P. F. (2006) in *Isotope Effects in Chemsitry and Biology* (Kohen, A., and Limbach, H.-H., Eds.), pp 861−873, CRC Taylor & Francis, Boca Raton, FL.

(35) Korzekwa, K. R., Trager, W. F., and Gillette, J. R. (1989) Theory for the observed isotope effects from enzymatic systems that form multiple products via branched reaction patyways: Cytochrome P-450. *Biochemistry 28*, 9012−9018.

(36) Darbyshire, J. F., Iyer, K. R., Grogan, J., Korzekwa, K. R., and Trager, W. F. (1996) Substrate probe for the mechanism of aromatic

hydroxylation catalyzed by cytochrome P450. *Drug Metab. Dispos. 24*, 1038−1045.
(37) Frantom, P. A., and Fitzpatrick, P. F. (2003) Uncoupled forms of tyrosine hydroxylase unmask kinetic isotope effects on chemical steps. *J. Am. Chem. Soc. 125*, 16190−16191.
(38) Tanaka, K., Nakai, Y., and Takahashi, H. (2011) Efficient NMR chiral discrimination of carboxylic acids using rhombamine macrocycles as chiral shift reagent. *Tetrahedron: Asymmetry 22*, 178−184.
(39) Johnson-Winters, K., Purpero, V. M., Kavana, M., Nelson, T., and Moran, G. R. (2003) 4-Hydroxyphenyl)pyruvate Dioxygenase from Streptomyces avermitilis: The Basis for Ordered Substrate Addition. *Biochemistry 42*, 2072−2080.
(40) Retey, J., Bartl, K., Ripp, E., and Hull, W. E. (1977) Stereospecificity of phenylpyruvate tautomerase. A convenient method for the preparation of chirally labelled phenylpyruvates. *Euro. J. Biochem. 72*, 251−257.
(41) Johnson, W. H., Jr., Czerwinski, R. M., Stamps, S. L., and Whitman, C. P. (1999) A kinetic and stereochemical investigation of the role of lysine-32 in the phenylpyruvate tautomerase activity catalyzed by macrophage migration inhibitory factor. *Biochemistry 38*, 16024−16033.
(42) O'Hare, H. M., Huang, F., Holding, A., Choroba, O. W., and Spencer, J. B. (2006) Conversion of hydroxyphenylpyruvate dioxygenases into hydroxymandelate synthases by directed evolution. *FEBS Lett. 580*, 3445−3450.
(43) Gunsior, M., Ravel, J., Challis, G. L., and Townsend, C. A. (2004) Engineering p-hydroxyphenylpyruvate dioxygenase to a p-hydroxymandelate synthase and evidence for the proposed benzene oxide intermediate in homogentisate formation. *Biochemistry 43*, 663−674.
(44) Brownlee, J., Johnson-Winters, K., Harrison, D. H. T., and Moran, G. R. (2004) The Structure of the Ferrous Form of (4−Hydroxyphenyl)pyruvate Dioxygenase from Streptomyces avermitilis in Complex with the Therapeutic Herbicide, NTBC. *Biochemistry 43*, 6370−6377.